

Comparison of Mo/MgO and Mo/ γ -Al₂O₃ catalysts: impact of support on the structure and dibenzothiophene hydrodesulfurization reaction pathways

A. Heidarinasab¹ · M. Soltanieh¹ · M. Ardjmand¹ · H. Ahmadpanahi¹ · M. Bahmani¹

Received: 8 October 2015 / Revised: 5 January 2016 / Accepted: 8 February 2016 / Published online: 24 February 2016
© Islamic Azad University (IAU) 2016

Abstract The MgO and P₂O₅-promoted γ -Al₂O₃ supports with alkaline and acidic natures, respectively, were prepared, impregnated with Mo atoms, and compared for dibenzothiophene (DBT) hydrodesulfurization (HDS) reaction. Ultraviolet spectroscopy and the principal component analysis were used to identify the impact of the supports on the reaction pathways. The catalysts were characterized by BET surface analysis, X-ray diffraction, temperature-programmed reduction, Fourier transform infrared, and X-ray photoelectron spectroscopy. The γ -Al₂O₃-supported catalyst favors the hydrogenation pathway relative to the MgO-supported catalyst, which facilitates the direct desulfurization route. The different performance was attributed to the dissimilar Mo phases that emerged during the activation procedure. The activation under sulfo-reductive condition changed the Mo atoms on γ -Al₂O₃ support into the sulfide phase while extra oxidation took place for the MgO-supported catalyst. The migration and consumption of loosely bonded bulk oxygen atoms with under-coordinated Mo atoms on the MgO support were introduced as a possible reason for such extra oxidation. DFT calculations predicted an interaction between the Mo/MgO catalyst and DBT via the electron donation from the catalyst oxygen atoms to the aromatic rings, resulting in weakening and breaking of the C–S bonds. In spite of the higher resistance of the MgO-supported catalyst toward coking and its superior activity, its lower hydrogenation capability suggested using a dual-function catalyst. Accordingly, two catalysts were mixed

and the synergism was observed in the HDS reaction of thiophene.

Keywords DFT · Predominance diagram · Principal component analysis · Reaction mechanism · Synergism · Thiophene

Introduction

The problem of deep removal of sulfur has become more serious due to the increasingly lower limits of sulfur content that are permitted by regulatory specifications to be in finished fuel products and the steadily higher sulfur content in the crude oil. Desulfurization methods, including various approaches such as adsorptive desulfurization (Saleh and Danmaliki 2015; Ahmed and Jhung 2016), oxidative desulfurization (Fox et al. 2015), biodesulfurization, chlorinolysis, and use of supercritical water (Javadli and Klerk 2012), have been introduced to meet the challenges of producing ultra-clean fuels at affordable prices. Although these methods are very promising for removing the refractory sulfur or nitrogen compounds at ambient temperature and pressure, hydrodesulfurization (HDS) is the most common method used in the petroleum industry to reduce the sulfur content of fuel products.

The HDS catalysts, which are generally composed of bimetal sulfides of CoMo and NiMo supported on alumina, play a very important role in decreasing sulfur in petroleum products, especially for producing sub-10 ppm diesel fuels (Coelho et al. 2015; Nakano et al. 2013; Villalón et al. 2015). In the petroleum refining industry and particularly from a commercial point of view, preparing and developing catalysts with high activity and high stability are of great interest for improving the performance of HDS process.

✉ M. Bahmani
m_bahmani_b@yahoo.com

¹ Department of Chemical Engineering, Science and Research Branch, Islamic Azad University, Tehran, Iran

Preparing an effective catalyst requires knowledge about the origins of the different functions of the catalyst and their dependence on the nature of the support, their compositions, and other variables.

The support plays an important role in determining the activity of the supported catalytic phase (Breysse et al. 2008; Pour et al. 2010; Ninh et al. 2011; Roukoss et al. 2009) and can significantly influence the catalytic characteristics. Various supports have been utilized for HDS reactions, including single and mixed metal oxides (Breysse et al. 2008), carbon (Babich and Moulijn 2003; Joshi et al. 2008) and zeolites (Al Bogami and de Lasa 2013; Acuña et al. 2015). In addition, most of the supports studied to date have been acidic in nature. A direct relationship has been found between the acidity of the support and its activity (Breysse et al. 2008; Chen et al. 2013). However, studies have indicated that alkaline MgO is as active as (or sometimes even more active than) acidic supports (Chary et al. 1991; Klicpera and Zdrzil 2002). In addition, the higher resistance of MgO-supported catalyst toward coking may facilitate operation at low or moderate pressures. However, the low specific surface area and low textural stability of magnesia have restricted its use as a support for HDS reactions (Zdrzil and Klicpera 2001; Solis et al. 2004). To overcome these limitations, modifying the composition of the support with MgO is regarded as the most economical and promising approach. Introducing the MgO on the formulation of Al_2O_3 not only promotes the reaction considerably, but also improves the stability of the catalyst (Wu et al. 2009). In addition, it can hinder the hydrogenation of unsaturated compounds, which are the fractions of greater value in petroleum products (Chary et al. 1991; Zdrzil and Klicpera 2001; Klicpera and Zdrzil 2002; Solis et al. 2004; Wu et al. 2009). The interest then rests in the way an alkaline support such as MgO influences the activity of the catalyst. Adjustment of the total number of acid sites and consequent reduction in the hydrocracking reactions (Kumar et al. 2004; Solis et al. 2007), improvements in dispersion of Mo atoms due to their stronger interaction with the support (Kumar et al. 2004; Rana et al. 2007; Solis et al. 2007; Trejo et al. 2008), and delay of the sulfidation of promoter atoms due to the formation of polymolybdates (Wu et al. 2009; Rana et al. 2007; Trejo et al. 2008; Cervantes et al. 2013) were introduced as the most important features of magnesia in the formulation of the mixed supports.

Although highly advanced techniques were used in previous studies to characterize the catalysts in the oxide form, the lack of knowledge concerning the activated and sulfide forms of the catalysts convinced us to address that topic and concentrate on the final structure of these catalysts along with their possible influences on the reaction mechanisms. In this regard, alkaline (MgO) and acidic

(P_2O_5 -promoted $\gamma\text{-Al}_2\text{O}_3$) supports were impregnated with Mo atoms and compared for HDS reaction pathways using ultraviolet (UV) spectroscopy and principal component analysis (PCA) methods. The simple-to-use multivariate methods such as PCA (Martens and Naes 1989) have frequently been applied to mixtures without resorting to time-consuming chemical separation like chromatography. Other types of analysis, including Brunauer–Emmett–Teller (BET) surface analysis, temperature-programmed reduction (TPR), X-Ray photoelectron spectroscopy (XPS), X-Ray powder diffraction (XRD), and bulk elemental analysis, were also used to characterize the activated and non-activated catalysts. Density functional theory (DFT) studies were performed as well to predict the reaction mechanisms. The research of this study was carried out in the period from January to July 2015 at the Central Lab of Bandar Abbas Oil Refinery in Bandar Abbas, Iran.

Materials and methods

Preparation of the catalysts

The two MgO supports that were used in this study were prepared from dehydration of $\text{Mg}(\text{OH})_2$ (Merck) at 800 °C under static air (noted MgO) and under vacuum condition (noted V–MgO). Highly acidic $\gamma\text{-Al}_2\text{O}_3 + 3 \text{ wt}\% \text{ P}_2\text{O}_5$ (noted $\gamma\text{-Al}_2\text{O}_3$) was prepared using the sol–gel method as described elsewhere (Rashidi et al. 2013). After this, 1.8 g of these supports was impregnated with 10 mL aqueous solution containing 0.37 g of ammonium hepta molybdate (BDH) using the incipient wetness technique so the catalysts contained 10 wt% Mo. The impregnated catalysts obtained in this fashion were dried at 120 °C for 24 h and then calcined for 4 h in air at 550 and 400 °C for the MgO- and $\gamma\text{-Al}_2\text{O}_3$ -supported catalysts, respectively. A NiMoP/ Al_2O_3 (3.0 wt% Ni, 12.0 wt% Mo, and 2.0 wt% P) commercial catalyst with a bulk density of 0.64–0.71 g/cm^3 was used in the HDS experiments. The textural properties and Mo content of the catalysts are given in Table 1. (The detailed characterization and catalytic behavior of the commercial catalyst have not been performed in this study; it has only been used to compare the activity of the catalysts. In addition, the V–MgO support has been used only to compare the preparation effect of the MgO support, and limited number of characterization techniques was used for this support in this study.)

Reaction tests

The activities of the catalysts for dibenzothiophene (DBT) HDS reactions were evaluated at different weight times (0,

Table 1 Textural properties of as prepared catalysts, S-to-Mo ratio of the pre-activated catalysts, total carbon of used catalysts, and catalytic activities for DBT conversion

Catalyst	Mo content (wt%)	S _{BET} (m ² /g)	Pore volume (cm ³ /g)	Average pore diameter (Å)	Activation gas stream	S/Mo ratio of activated catalyst ^a	DBT conversion ^b (%)	Total carbon of used catalyst (wt%)
Comm. catalyst	12.02	199.0	0.312	64.0	DMDS + H ₂	2.1	88.0	9.6
Mo/V–MgO	9.66	20.6	0.108	126	DMDS + H ₂	0.6	72.0	4.6
Mo/MgO	9.53	19.9	0.091	120	H ₂	0.0	96.5	0.2
					DMDS + H ₂	0.0	96.5	0.6
					H ₂ S + H ₂	0.04	96.3	0.3
Mo/γ-Al ₂ O ₃	10.18	186.0	0.300	78	H ₂	0.0	42.0	12.6
					DMDS + H ₂	2.0	78.0	8.9
					H ₂ S + H ₂	2.1	77.7	8.6

^a The catalysts were activated at 350 °C for 8 h under a flow of defined activation gas stream

^b The catalytic activities were evaluated at 60 gr.min/mmol reaction weight time under atmospheric pressure at 320 °C

6.0, 9.0, 12.0, 15.0, 20.0, 30.0, and 60.0 g.min/mmol), at 320 °C in a fixed bed reactor operating at atmospheric pressure. The catalysts were activated at 350 °C for 8 h under a flow of dimethyl disulfide (1 Vol % in isooctane)/H₂ mixture. During each run, 0.2 g of the catalyst was loaded into the reactor, with glass wool used as a diluent. The ratio of H₂ gas to oil was kept constant (500 Nml H₂/ml oil) across all experiments. A total of 4312.5 mg DBT (Merck) was dissolved in 1 kg isooctane (Ubachem) to yield the 750 ppm sulfur. The products were analyzed for total sulfur content using Antek (PAC; Houston, Texas, US).

PCA methods

The samples for each different run were collected after 24 h (all reactions became steady after about 8 h). In a typical analysis of the samples, 1.0 mL of the HDS products was diluted with 49.0 mL isooctane and then pipetted into a 3.5 mL quartz bulb. The absorbance data of the solution were measured immediately. All spectral data were collected simultaneously from 190 to 300 nm every 1 nm, using isooctane as a blank (Gupta et al. 2011a; Saleh and Gupta 2011; Gupta et al. 2012). Absorption data acquisition was performed through UV–Vis DR-4000U spectrophotometer (HACH; Loveland, Colorado, USA). All assays were performed at room temperature. The data matrixes obtained from the measurements were then resolved using a PCA method to evaluate the concentration profiles and pure spectra of the chemical compounds simultaneously from decomposition of a multivariate multi-component experimental data matrix (Elbergali et al. 1999; Meloun et al. 2000; Wang et al. 2008; Birkholz and Schlegel 2012). PCA is a commonly used technique that

can resolve multi-component mixtures into a simple model consisting of a composition-weighted sum of the signals of the pure compounds (Jolliffe 2002). Microsoft Excel (version 2007; Microsoft, Redmond, Washington, USA) and Minitab version 15 statistical software (Minitab; State College, Pennsylvania, USA) were used to refine the pure spectra and concentration profiles.

Characterization of the catalysts

To define the nature of the acidity or alkalinity of the supports, IR spectra were recorded on a JASCO FTIR-4100 spectrometer using its diffuse reflectance accessory (JASCO Analytical Instruments; Easton, Maryland, US) with a resolution of 4 cm⁻¹ (Saleh 2011, 2015b; Saleh et al. 2011; Saleh and Gupta 2012a). The catalysts were degassed at 300 °C for 1 h under vacuum conditions, followed by adsorption of pyridine at room temperature and evacuation at 150 °C for acidity and adsorption of nitrobenzene at 70 °C for alkalinity (Tamura et al. 2012).

The XRD patterns of the samples were recorded by Equinox-2000 (INEL; Ardenay, France) using Cu Kα radiation. The accelerating voltage and applied current were 40 kV and 30 mA, respectively (Saleh and Gupta 2012b, c; Gupta et al. 2011b, c).

The XPS analyses of the catalysts were carried out using a VG ESCALAB spectrophotometer (VG Systems Inc.; Renton, Washington, USA) equipped with a monochromatic AlKα X-ray source (1486.6 eV). During the measurement, the base pressure of the system was around 5*10⁻¹⁰ mbar. C 1 s (248.6 eV) was used as the reference to correct the binding energy (Gupta and Saleh 2013).

The specific surface area, pore volume, and porosity distribution of the catalysts were obtained from nitrogen



adsorption–desorption isotherms, determined at 77°K with an ASAP 2010 apparatus. Surface areas were calculated by the BET method, and the pore size distribution and total pore volume were determined by the Barrett–Joyner–Halenda (BJH) method. Prior to adsorption, the samples were out-gassed at 300 °C for 4 h under a residual pressure of 10^{-4} mmHg (Saleh 2015b; Saleh and Gupta 2014, Saleh and Gupta 2011; Gupta et al. 2013).

Temperature-programmed reduction (TPR) experiments were carried out in a micro-reactor system using online gas chromatography. Samples of 50 mg were first treated in argon at room temperature for 1 h. The samples were then reduced in an H_2/Ar mixture (with a molar ratio of 0.05 and a total flow of 30 mL/min) and heated at a ramping rate of 10 °C/min to a final temperature of 1000 °C.

The concentration of Mo in sulfuric acid digested catalysts was determined by atomic absorption technique with contrAA 700 (Analytik Jena AG; Jena, Germany).

Multi EA 4000 (Analytik Jena AG; Jena, Germany) was used to determine the concentration of the total sulfur and total carbon in activated and used catalysts, respectively.

Theoretical calculations

A detailed structural study of DBT and a simplified structure of $MgO-MoO_3$ were carried out using ab initio quantum chemical methods. The electronic structure of these compounds was studied within the frame of the hybrid DFT. The well-known B3LYP hybrid exchange–correlation functional (Becke 1993, 1988) was used in combination with LanL2DZ basis sets for Mo and Mg atoms and 6-31G (d,p) basis sets for other atoms. The DBT molecule was fully optimized from starting geometries, while the geometry of $MgO-MoO_3$ was kept constant at its experimental values (Gemmi et al. 2015). All the calculations were performed with the Gaussian 98 package (Frisch et al. 1998). The electronic structures that were obtained and analyzed are the widely used highest occupied molecular orbital (HOMO) and lowest unoccupied molecular orbital (LUMO).

In addition, thermodynamic calculations were carried out using HSC Chemistry 6.0 software to study the predominance diagram for Mo atoms on a Mo–Mg–O system.

Results and discussion

Characterization of the supports and catalysts

FTIR spectroscopy results

To define the qualitative nature of the alkalinity and the acidity of the supports, IR experiments were performed

using nitrobenzene and pyridine as probe molecules, respectively (Tamura et al. 2012). The results clearly demonstrate the acidic nature of $\gamma-Al_2O_3$ and the alkalinity of MgO (Fig. 1).

XRD results

The supports were characterized using XRD (Fig. 2a). The lower 2-theta ranges are only shown for the activated and non-activated catalysts because of the similarities in XRD patterns at higher 2-theta ranges (Fig. 2b, c). The V–MgO support shows exactly the same XRD pattern as that of the MgO support and has, therefore, not been shown in Fig. 2.

Impregnation leads to the development of a number of new peaks in both catalysts within 20 to 35 2-theta ranges in response to the presence of Mo atoms. However, these peaks disappeared for the $\gamma-Al_2O_3$ -supported catalyst upon activation, while those of the MgO-supported catalyst remained unchanged.

TPR results

The TPR profiles of the oxide catalysts are shown in Fig. 3. The TPR profiles of the $Mo/\gamma-Al_2O_3$ record two peaks at 465 and 535 °C, respectively. The low-temperature reduction peak can be attributed to the first step in the reduction ($Mo^{+VI} + 2e^- = Mo^{+IV}$) of an octahedral Mo species well dispersed on the support. The high-temperature reduction peak can be ascribed to the second step in the reduction of octahedral Mo species of different degrees of agglomeration ($Mo^{+IV} + 4e^- = Mo^0$) and also to the first step in the reduction of isolated tetrahedral Mo^{6+} species that interact strongly with the support. For the MgO-supported catalyst, there are two peaks at 750 and 920 °C, respectively. It is believed that there is a strong interaction between MgO support and Mo atoms. The TPR peaks below 800 °C can be assigned to the reduction of tetrahedrally coordinated Mo^{6+} in MoO_4^{2-} species

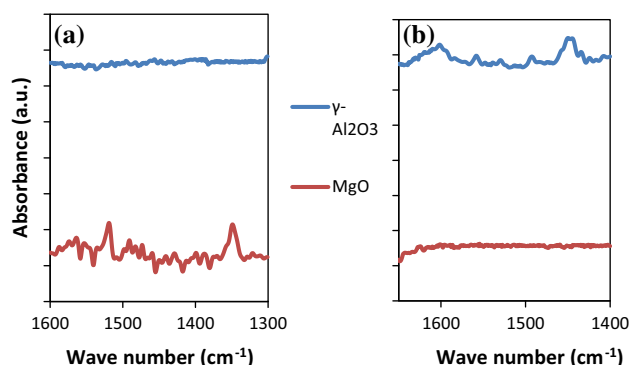


Fig. 1 FTIR spectra of **a** nitrobenzene and **b** pyridine adsorbed on MgO and $\gamma-Al_2O_3$ supports

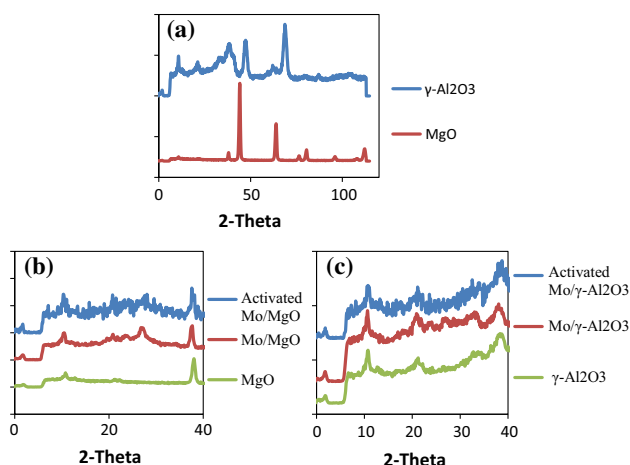


Fig. 2 XRD patterns of **a** MgO and γ -Al₂O₃, **b** MgO, Mo/MgO, and activated Mo/MgO, and **c** γ -Al₂O₃, Mo/ γ -Al₂O₃, and activated Mo/ γ -Al₂O₃

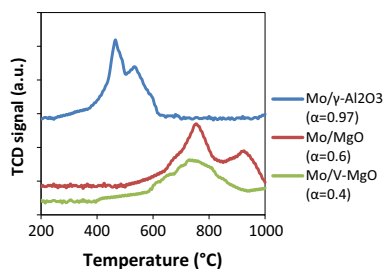


Fig. 3 Mo (3d), S (2p), and O (1s) XPS spectra for activated and non-activated Mo/MgO and Mo/ γ -Al₂O₃ catalysts

(MgMoO₄) and the one at 920 °C can be assigned to the reduction of Mo⁶⁺ in crystalline MgMoO₄ phase (Lee et al. 2004). In the case of the V–MgO support, the first peak was broadened and the second peak disappeared.

Figure 3 also shows results from the quantification of the total amount of hydrogen consumed during the reduction of the catalysts. This figure demonstrates that the reduction of the MgO-supported catalysts proceeds with lower hydrogen consumption than that of the γ -Al₂O₃-supported catalyst. The degree of reduction (α) in these catalysts (determined from H₂ consumption measured for each sample and the theoretical value corresponding to their complete reduction), indicates that most of the Mo oxide species on MgO supports were not reduced in the TPR experiments. The above results point out that using an alkaline support not only results in an increase in the temperature of the reduction of the Mo oxide species, but also makes their reductions less complete. This observation can be explained by the strong interaction of Mo oxide species in the alkaline catalysts and the increase in the proportion of tetrahedrally coordinated Mo⁶⁺ ions that cannot be reduced in comparison with the corresponding octahedral ones in the acidic catalysts.

XPS results

It is widely accepted that supported Mo species are present on the surface of HDS catalysts in a highly dispersed state. Consequently, the use of bulk characterization techniques is not adequate in determining the chemical state of Mo-based catalysts. XPS provides interesting information concerning the state of highly dispersed catalysts and is a technique that has been used in similar studies to determine the extent and state of Mo sulfidation in the presence (Coulier et al. 2002; Fontaine et al. 2010) and absence (Muijsers et al. 1995; Saih and Segawa 2003) of promoter over different supports (Muijsers et al. 1995; Roukoss et al. 2009).

The XPS spectra of Mo (3d), S (2p), and O (1s) were obtained for the activated and the non-activated catalysts (Fig. 4). According to the S (2p) spectra of the catalysts, a sharp sulfur peak appears for the γ -Al₂O₃-supported catalyst after activation; in contrast, there is no trace of sulfur in the case of the activated MgO-supported catalyst. The Mo (3d) spectra reveal exactly the same oxidation state (Mo^{+VI} + Mo^{+V}) for both non-activated catalysts (Muijsers et al. 1995). However, the trend is not the same for activated catalysts; activation reduces the Mo species over γ -Al₂O₃ to Mo^{+IV}, while the MgO-supported catalyst not only shows no such reduction, but also shows extra oxidation compared with its non-activated counterparts. Activation made the O (1s) spectra of the γ -Al₂O₃-supported catalyst reduce both in amount and in binding energy; however, both of these increased for activated MgO-supported catalyst.

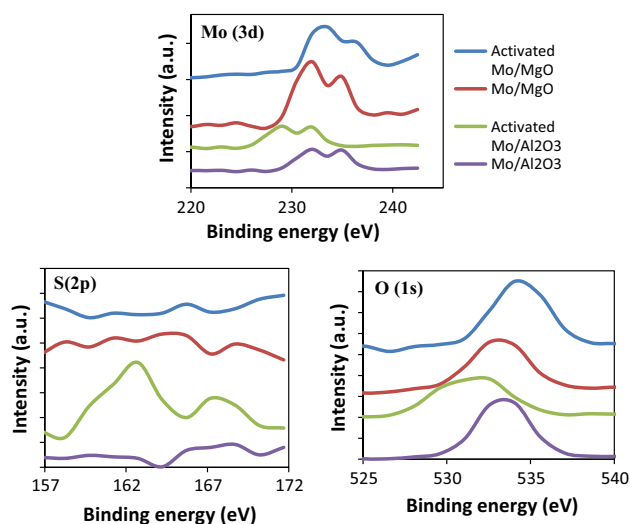


Fig. 4 TPR profiles and degree of the reduction of Mo oxide species (α) on Mo/MgO and Mo/ γ -Al₂O₃ catalysts

PCA assessments

The DBT HDS reaction was performed at different weight times over the Mo/MgO and Mo/ γ -Al₂O₃ catalysts; Fig. 5a shows the UV absorption spectra for all reaction products. Afterward, PCA was applied to estimate the number and spectral profiles of the components. The results of this process (Fig. 5b) indicate the major constitutive principal components (PCs) of the reaction products. The next step was to define the concentration profiles for each of the PCs. In this regard, an iterative optimization procedure was used to minimize the error-related matrix (E) in Eq. 1. In this equation, D, S^T, and C are related to the UV data matrix

$$D = CS^T + E \quad (1)$$

The PCA results indicate the presence of only two PCs for the reaction products over the Mo/MgO catalyst. PC1 has exactly the same UV pattern as DBT (Talrose et al. 2015) and as a consequence reflects the characteristics of the reactant. However, due to the absence of a peak around 235 nm (characteristic of all thiophene-containing compounds), PC2 can be treated as a pseudo-component representing the desulfurized DBT products. The exact characterization of this PC is impossible because most of the candidate reaction products (such as biphenyl and cyclohexylbenzene) have similar UV patterns (Talrose et al. 2015).

In contrast to the Mo/MgO catalyst, the PCA of the reaction products over the Mo/ γ -Al₂O₃ catalyst yields three major PCs. PC1 and PC2 are similar to those of Mo/MgO; however, the third PC, with a distinct absorption peak around 235 nm, can be a thiophene-containing molecule (Talrose et al. 2015) or simply a hydrointermediate DBT (HIDBT) component.

The results in Fig. 5c are not the exact concentration profiles, but rather their trends; accordingly, they cannot be used to define the kinetic parameters. Estimation of the exact kinetic parameters requires the actual concentration profiles. Fortunately, because of the irreversibility of the HDS reaction, the estimation of the exact concentration of the product molecule (PC2) is not required and its trend seems to be representative enough to account for its behavior. Nonetheless, determining the exact concentration of PC1 and PC3 is critical to explain the kinetics.

To quantify the UV data results in Fig. 5a and according to the previous paragraphs, DBT was selected to calibrate PC1. In addition, thiophene with a UV pattern similar to HIDBT was selected instead of PC3. The concentration of DBT was calibrated at the absorbance at 286 nm, and the DBT and thiophene concentrations were summed at 235 nm. The sulfur concentration of each component was used in the calibration in the place of the concentrations of the components themselves. This substitution is necessary since the exact nature of the HIDBT is unknown, and use of the thiophene instead of HIDBT is controversial.

The concentration profiles obtained with calibration are shown in Fig. 5d. The uncertainties for concentrations were estimated to be approximately 5.4 % with a confidence level of 95 % and coverage factor $K = 2$. The estimated uncertainties were mainly originated from the errors caused by PCA method; there were also some minor experimental uncertainties (dilution and repeatability) which were included in estimated uncertainties (Coleman et al. 1999).

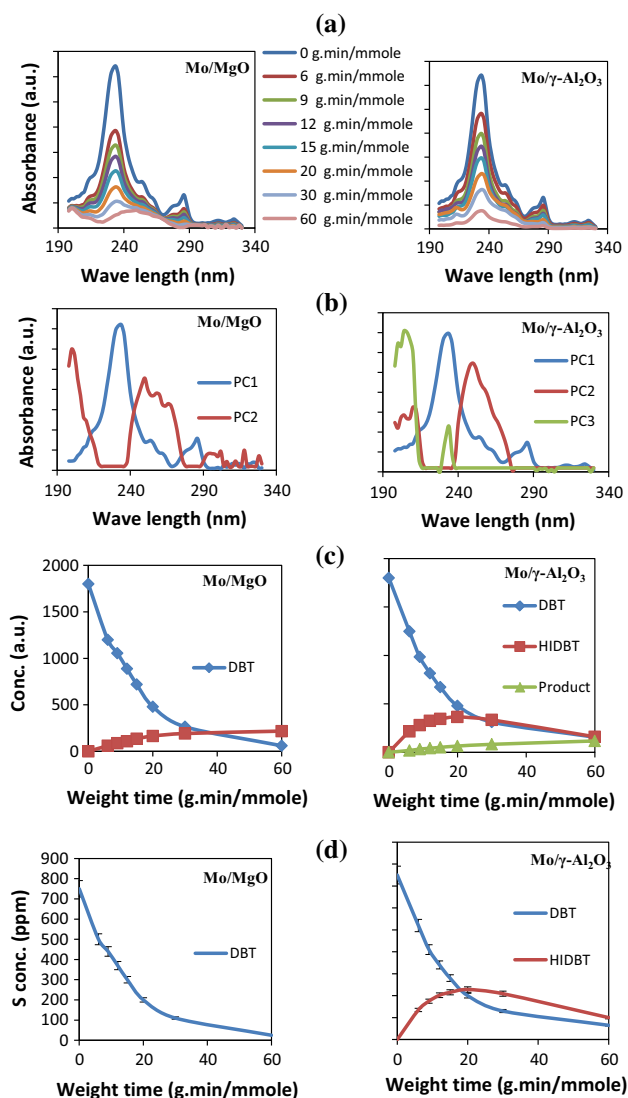


Fig. 5 a UV data results at different reaction weight times, b constituent PCs of the HDS reaction products, c concentration profiles of the PCs obtained with PCA methods, and d sulfur concentration profiles of the HDS reaction products obtained with calibration of UV data results (the error bars indicate the estimated uncertainties)

Table 2 Total sulfur concentrations of HDS reaction products on catalysts at different weight times (the data in brackets show the total sulfur concentrations obtained with calibration of UV data results)

Catalyst	Reaction weight times (g.min/mmol)							
	0	6.0	9.0	12.0	15.0	20.0	30.0	60.0
Mo/ γ -Al ₂ O ₃	761 (750)	659 (655)	588 (585)	551 (542)	498 (495)	433 (428)	348 (339)	167 (165)
Mo/MgO	761 (750)	504 (500)	441 (440)	376 (370)	304 (300)	208 (200)	119 (110)	26 (25)

Comparing the results in Fig. 5c and d indicates that great compatibility between the two methods exists with respect to predicting the concentration profiles. Furthermore, the total concentrations of sulfurs obtained experimentally were compared with those from calibration (Table 2). Generally, extremely good agreement exists between the results, indicating the reliability and accuracy of the procedure in selecting and separating the components to regenerate the UV data results.

The effect of the activation gas stream

Three different gas streams—H₂, H₂S (1 %) + H₂, and DMDS (1 % in isooctane) + H₂—were used to investigate the effect of the activation atmosphere on the activity and the S-to-Mo ratio of the final catalysts. According to the results for the MgO-supported catalyst, no significant difference exists in the catalytic activity or in the S-to-Mo ratio of the final catalysts concerning the change in the activation gas stream (Table 1). In contrast, for the Mo/ γ -Al₂O₃ catalyst, although changing the sulfidation agent (DMDS or H₂S) has no marked influence, the absence of any sulfidation agent has a very profound effect on both the activity and the S-to-Mo ratio of the final catalysts.

DBT HDS reaction pathway

According to the PCA results, three components or pseudo-components take part in the HDS reaction over the Mo/ γ -Al₂O₃ catalyst: DBT, HIDBT, and the product. The concentration profiles of these components illustrate that the concentration declines for DBT and increases for the products (Fig. 5c). The zero slope of the product's concentration profile at the beginning of the reaction suggests that it is not a primary but a secondary product. In addition, the concentration profile of HIDBT behaves as an intermediate component. Therefore, a series reaction can be used to describe the DBT HDS reaction pathway over this

catalyst (Scheme 1a). Furthermore, the data in Fig. 5d were used to obtain the reaction rate constants by assuming a pseudo-first-order reaction rate, which is a common assumption for HDS reaction (Sun and Prins 2009; Baldivino et al. 2010).

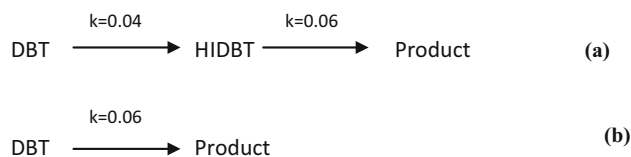
Unlike the γ -Al₂O₃-supported catalyst, the reaction on the Mo/MgO catalyst results in two components or pseudo-components: DBT and the product. The concentration decreases for DBT and increases for the product, with a nonzero slope at the beginning of the reaction. Therefore, in this case the product behaves as a primary product. Consequently, a simple direct reaction pathway can be proposed for this reaction (Scheme 1b). Similarly, the data in Fig. 5d were used to obtain the pseudo-first-order reaction rate constants.

It can be deduced that the HDS reaction proceeds through the hydrogenation pathway on the Mo/ γ -Al₂O₃ catalyst, with the hydrogenation step as the rate-determining step. In contrast, the MgO-supported catalyst favors the direct desulfurization pathway, collaborating with the previous reports (Chary et al. 1991; Zdrzil and Klicpera 2001; Klicpera and Zdrzil 2002; Solis et al. 2004; Wu et al. 2009). It should be stated that both pathways may participate in overall HDS reactions on both catalysts; however, because of the approximate nature of the PCA method, only the predominant pathways were detected.

Structural comparison of the catalysts

It is interesting to observe the origin of such a difference in the catalytic behavior of MgO- and γ -Al₂O₃-supported catalysts in cases where the active metal is the same. For this purpose, the structures of the activated and the non-activated catalysts were evaluated.

The XPS results (Fig. 4) and the values for the S-to-Mo ratio (Table 1) for the γ -Al₂O₃-supported catalyst show that the total sulfidation of Mo takes place in activation. The MoS₂ phase has, therefore, been substituted for the original MoO₃ phase. In addition, the XRD results indicate



Scheme 1 Reaction pathway and pseudo-first-order reaction rate constants (mmol/g.min) on **a** Mo/ γ -Al₂O₃ and **b** Mo/MgO catalyst for HDS of DBT

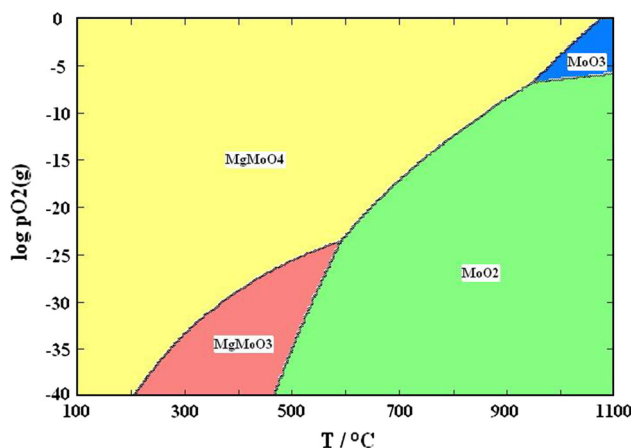


Fig. 6 Predominance diagram for Mo atoms on Mo–Mg–O system

that this substitution is accompanied by good distribution of the newly generated sulfide phase (Fig. 2).

Unlike the Mo/ γ -Al₂O₃ catalyst, the XPS results, the S-to-Mo ratio values, and the XRD results for the MgO-supported catalyst reveal that the Mo retains its oxide phase upon activation. In addition, according to the O (1 s) XPS results, not only does the reduction (and consequently the sulfidation of the Mo atoms) not occur, but extra oxidation takes place. In order to find out how the oxygen atoms influence the structure of the Mo/MgO catalyst, thermodynamic calculations were carried out to study the predominance diagram of Mo atoms on the Mo–Mg–O system (Fig. 6). It can be deduced from these results that the formation of oxygen-deficient structures is possible under oxygen-lean conditions. Therefore, the low degree of reduction values in TPR experiments (Fig. 3) for MgO-supported catalysts (especially for the Mo/V–MgO catalyst) may originate not only from their hard reducibility, but also from their under-stoichiometric structures. Consequently, it can be assumed that the activation under highly sulfo-reductive conditions causes some loosely bonded bulk oxygen species to migrate toward the surface and be consumed by under-coordinated Mo atoms. This phenomenon can explain the extra oxidation of Mo atoms during the activation procedure (Fig. 4). However, under-

coordinated Mo atoms on V–MgO support (owing to the lack of loosely bonded oxygen atoms) have no chance of being saturated with oxygen atoms and, consequently, of being coordinated with sulfur atoms. This could be the cause of partial sulfidation of the Mo/V–MgO catalyst (Table 1) during the activation procedure.

In conclusion, owing to the non-sulfidability of the MgO-supported catalyst, the activity of this catalyst is independent of the pre-activation gas stream (Table 1). In contrast, the activity of the Mo/ γ -Al₂O₃ catalyst depends heavily on the presence or absence of any sulfidizing agent; however, this dependence on the kind of sulfidizing agent is insignificant.

Overall, the dissimilar Mo phases that emerged from the two different supports could be the reason for the observed discrepancies that were observed between the reaction pathways. Similar correlations between the reaction pathways and the acidity or alkalinity of the catalyst using fluorine, phosphorus, and ammonia in catalyst formulations have been reported in previous studies (Moon 2003).

DBT HDS reaction mechanism

The well-known donation and back-donation mechanism, involving donation from a thiophene-containing compound, back-donation from the catalyst surface, and destruction of the aromatic character of the molecule, has already been reported (Borges et al. 2007) in describing the HDS reaction mechanism on the MoS₂ phase. In fact, the semi-metal MoS₂ phase, with 0.9 eV band gap energy (Ahmad and Mukherjee 2014), provides well-known *rim* sites, causing the parallel adsorption of DBT molecules and activation of the hydrogenation pathway (Topsøe et al. 2005; Lauritsen et al. 2006). However, owing to the low metallic nature of the MoO₃ phase, with 3.1 eV band gap energy (Patil et al. 2011), the HDS reaction mechanism on the Mo/MgO catalyst cannot be explained by the donation and back-donation mechanism.

The nature of the interaction between DBT molecules and the simplified structure of the Mo/MgO catalyst was envisioned at a molecular level with the help of frontier molecular orbital calculated using the DFT approach (Saleh et al. 2013; Saleh et al. 2014; Al-Saadi et al. 2013). Figure 7 shows the HOMO and LUMO predicted at the DFT/B3LYP level of theory in combination with LanL2DZ basis sets for Mo and Mg atoms and 6-31G (d,p) basis sets for other atoms. The HOMO and LUMO can be perceived as the electron-donor and electron-acceptor parts, respectively, of the molecule. The figure shows that, for the catalyst, only the HOMO localized on the oxygen atoms is

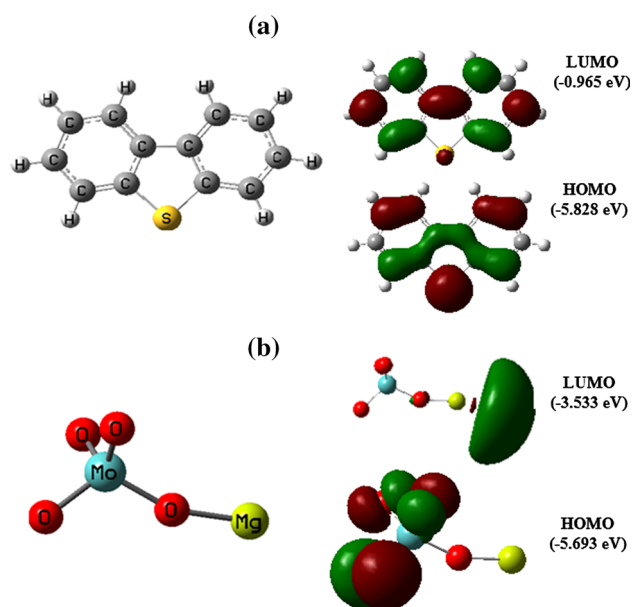


Fig. 7 Frontier molecular orbitals (HOMO and LUMO) and corresponding energies for **a** DBT and **b** MgO–MoO₃ calculated at the DFT/B3LYP level of theory

accessible for the reactants. In the case of the DBT molecule, the HOMO lobe is localized on the sulfur heteroatom and the LUMO lobe is localized on carbon atoms. Therefore, an interaction can take place between the catalyst surface and the reactant through the electron donation from the catalyst oxygen atoms to the aromatic rings, resulting in weakening and breaking of the C–S bonds. This phenomenon may be helpful during the desulfurization of highly difficult molecules (such as 4,6 DMDBT), where the sulfur does not contribute directly to the adsorption and the steric hindrance caused by the adjacent methyl groups does not inhibit the adsorption or desulfurization processes.

Synergism

The data in Table 1 reveal the superior activity of the Mo/MgO catalyst in the desulfurization reaction compared to the γ -Al₂O₃-supported and commercial catalysts at atmospheric pressure. The alkalinity of this catalyst also resulted in its higher resistance to coking (Table 1). However, it lacks hydrogenation capability. Hydrogenation (or at least partial hydrogenation) is a highly effective method for improving the reactivity of extremely hard sulfur-containing molecules in desulfurization reactions (Delmon 1993). Therefore, it is expected that use of a dual-function catalyst with the advantages of both phases will be highly effective

in desulfurizing hard reactive components: MoS₂ for hydrogenation and MoO₃ for desulfurization.

This synergistic effect was evaluated for the thiophene molecule. Thiophene, which has a lower electron density over sulfur heteroatom, has an extremely low activity toward desulfurization at atmospheric pressure. The activation of this molecule is only possible through hydrogenation or at least partial hydrogenation (Kilanowski et al. 1978; Ma et al. 1995). Both catalysts have relatively low activity toward the desulfurization of this molecule (25 % for the Mo/MgO catalyst and 43 % for the Mo/ γ -Al₂O₃). However, physically mixing the two catalysts (50 wt% Mo/MgO + 50 wt % Mo/ γ -Al₂O₃) significantly improves thiophene reactivity (75 %). This synergism could be a reason for the improvements that were previously observed in the catalytic activity using MgO + γ -Al₂O₃ as a support (Rana et al. 2007; Trejo et al. 2008).

Conclusion

This study evaluated the catalytic behavior of Mo for desulfurization reactions over supports with different acidic or alkaline natures. MgO- and P₂O₅-promoted γ -Al₂O₃ supports were selected as alkaline and acidic supports, respectively. Using PCA in reaction pathway assessments showed major differences between these two catalysts with respect to reaction pathway preference. The reaction over the acidic support proceeds through the hydrogenation pathway, whereas the alkaline support favors a direct desulfurization pathway. Different emerged Mo phases over these supports could be the main reason for these findings. Activation resulted in the Mo over γ -Al₂O₃ changing into the MoS₂ phase while, for the MgO-supported Mo species, not only does the reduction (and consequently the sulfidation) not occur, but extra oxidation takes place. The migration and consumption of loosely bonded bulk oxygen atoms with under-stoichiometric Mo atoms during the activation procedure may be the reason for such extra oxidation. The strong interaction between the Mo/MgO catalyst and the DBT through the electron donation from the catalyst oxygen atoms to the aromatic rings was considered as a possible HDS reaction mechanism, resulting in weakening and breaking of the C–S bonds.

The alkaline MgO support resulted in superior activity of the Mo catalyst and extremely low coking. However, this catalyst's lack of capability for hydrogenation suggests the use of a dual-function catalyst to benefit from the

advantages of both phases in one catalyst. Synergism was observed for the desulfurization of thiophene when the two catalysts were physically mixed.

Acknowledgments The authors sincerely thank Science and Research Branch of Islamic Azad University (SRBIAU) and the Central Lab of Bandar Abbas oil refinery for their support.

References

- Acuña R, Zepeda TA, Muñoz EM, Nava R, Loricera CV, Pawelec C (2015) Characterization and HDS performance of sulfided CoMoW catalysts. *Fuel* 149:149–161
- Ahmad S, Mukherjee S (2014) A comparative study of electronic properties of bulk MoS₂ and its monolayer using DFT technique: application of mechanical strain on MoS₂ monolayer. *Graphene* 3:52–59
- Ahmed I, Jhung SH (2016) Adsorptive desulfurization and denitrogenation using metal-organic frameworks. *J Hazard Mater* 301:259–276
- Al Bogami S, de Lasa H (2013) Catalytic conversion of benzothiophene over a H-ZSM5 based catalyst. *Fuel* 108:490–501
- Al-Saadi AA, Saleh TA, Gupta VK (2013) Spectroscopic and computational evaluation of cadmium adsorption using activated carbon produced from rubber tires. *J Mol Liq* 188:136–142
- Babich IV, Moulijn JA (2003) Science and technology of novel processes for deep desulfurization of oil refinery streams: a review. *Fuel* 82:607–631
- Baldovino VG, Giraldo S, Centeno A (2010) Hydrotreating of heavy gas oil using CoMo/-Al₂O₃ catalyst prepared by equilibrium deposition filtration. *Fuel* 89:1012–1018
- Becke AD (1988) Density-functional exchange-energy approximation with correct asymptotic behavior. *Phys Rev A* 38:3098
- Becke AD (1993) Density-functional thermochemistry: III, the role of exact exchange. *J Chem Phys* 98:5648
- Birkholz AB, Schlegel HB (2012) Coordinate reduction for exploring chemical reaction paths. *Theor Chem Acc* 131:1170
- Borges I Jr et al (2007) Density functional theory molecular simulation of thiophene adsorption on MoS₂ including microwave effects. *J Mol Struct: THEOCHEM* 822:80–88
- Breyse M, Grantel C, Afanasiev P, Blanchard J, Vriant M (2008) Recent studies on the preparation, activation and design of active phases and supports of hydrotreating catalysts. *Catal Today* 130:3–13
- Cervantes M, Albiter M, Larios A, Balbuena B, Perla B, Valencia J (2013) Experimental and theoretical study of NiMoW, NiMo, and NiW sulfide catalysts supported on an Al–Ti–Mg mixed oxide during the hydrodesulfurization of dibenzothiophene. *Fuel* 113:733–743
- Chary KVR, Ramakrishna H, Rao KSR, Murali Dhar G, Kanto Rao P (1991) Hydrodesulfurization on MoS₂/MgO. *Catal Lett* 10:27–34
- Chen W, Mauge F, Van Gestel J, Nie H, Li D, Long X (2013) Effect of modification of the alumina acidity on the properties of supported Mo and CoMo sulfide catalysts. *J Catal* 304:47–62
- Coelho TL, Licea YE, Palacio LA, Faro AC Jr (2015) Heptamolybdate-intercalated CoMgAl hydrotalcites as precursors for HDS-selective hydrotreating catalysts. *Catal Today* 250:38–46
- Coleman HW, Steele J, Glenn W (1999) Experimentation and uncertainty analysis for engineers. Wiley, New York
- Coulier L, Kishan G, Van Veen JAR, Niemantsverdriet JW (2002) Influence of support-interaction on the sulfidation behavior and hydrodesulfurization activity of Al₂O₃-Supported W, CoW, and NiW model catalysts. *J Phys Chem B* 106:5897–5906
- Delmon B (1993) New technical challenges and recent advances in hydrotreatment catalysis: a critical updating review. *Catal Lett* 22:1–32
- Elbergali A, Nygren J, Kubista M (1999) An automated procedure to predict the number of components in spectroscopic data. *Anal Chim Acta* 379:143–158
- Fontaine C, Romero Y, Daudin A, Devers E, Bouchy C, Brunet S (2010) Insight into sulphur compounds and promoter effects on Molybdenum-based catalysts for selective HDS of FCC gasoline. *Appl Catal A: General* 388:188–195
- Fox BR et al (2015) Enhanced oxidative desulfurization in a film-shear reactor. *Fuel* 156:142–147
- Frisch MJ et al (1998) Gaussian 98, revision A.7. Gaussian, Inc., Pittsburgh, PA
- Gemmi M, La Placa MG, Galanis AS, Rauch EF, Nicolopoulos S (2015) Fast electron diffraction tomography. *J Appl Cryst* 48:718–727
- Gupta VK, Saleh TA (2013) Sorption of pollutants by porous carbon, carbon nanotubes and fullerene—an overview. *Environ Sci Pollut Res* 20:2828–2843
- Gupta VK, Jain R, Saleh TA, Nayak A, Malathi S, Agarwal S (2011a) Equilibrium and thermodynamic studies on the removal and recovery of safranin-T dye from industrial effluents. *Sep Sci Technol* 46:839–846
- Gupta VK, Agarwal S, Saleh TA (2011b) Synthesis and characterization of alumina-coated carbon nanotubes and their application for lead removal. *J Hazard Mater* 185:17–23
- Gupta VK, Agarwal S, Saleh TA (2011c) Chromium removal by combining the magnetic properties of iron oxide with adsorption properties of carbon nanotubes. *Water Res* 45:2207–2212
- Gupta VK, Ali I, Saleh TA, Nayak A, Agarwal S (2012) Chemical treatment technologies for waste-water recycling—an overview. *RSC Adv* 2:6380–6388
- Gupta VK, Kumar R, Nayak A, Saleh TA, Barakat MA (2013) Adsorptive removal of dyes from aqueous solution onto carbon nanotubes: a review. *Adv Colloid Interface Sci* 193–194:24–34
- Javadli R, Klerk A (2012) Desulfurization of heavy oil. *Appl Petrochem Res* 1:3–19
- Jolliffe IT (2002) Principal component analysis, 2nd edn. Springer-Verlag, New York
- Joshi YV, Ghosh P, Daage M, Delgass N (2008) Support effects in HDS catalysts: DFT analysis of thiolysis and hydrolysis energies of metal-support linkages. *J Catal* 257:71–80
- Kilanowski DR, Teeuwen H, De Beer VHJ, Gates BC, Schuit GCA, Kwart H (1978) Hydrodesulfurization of thiophene, benzothiophene, dibenzothiophene, and related compounds catalyzed by sulfided CoO + MoO₃/γ-Al₂O₃: low-pressure reactivity studies. *J Catal* 55:120–137
- Klicpera T, Zdrzil M (2002) Preparation of High-activity MgO-supported Co–Mo and Ni–Mo sulfide hydrodesulfurization catalysts. *J Catal* 206:314–320
- Kumar M, Aberuagba F, Gupta JK, Rawat KS, Sharma LD, Murali Dhar G (2004) Temperature-programmed reduction and acidic properties of molybdenum supported on MgO–Al₂O₃ and their correlation with catalytic activity. *J Mol Catal A* 213:217–223

- Lauritsen J, Vang R, Besenbacher F (2006) From atom-resolved scanning tunneling microscopy (STM) studies to the design of new catalysts. *Catal Today* 111:34–43
- Lee EK, Jung KD, Joo OS, Shul YG (2004) Catalytic activity of Mo/MgO catalyst in the wet oxidation of H₂S to sulfur at room temperature. *Appl Catal A: Gen* 268:83–88
- Ma X, Sakanishi K, Isoda T, Mochida I (1995) Quantum chemical calculation on the desulfurization reactivities of heterocyclic sulfur compounds. *Energy Fuels* 9:33–37
- Martens H, Naes T (1989) *Multivariate calibration*. Wiley, Chichester
- Meloun M, Apek J, Mikšik P, Brereton R (2000) Critical comparison of methods predicting the number of components in spectroscopic data. *Anal Chim Acta* 423:51–68
- Moon SH (2003) Effect of acidic and basic species on the hydrodesulfurization of methyl-substituted dibenzothiophenes. *Catal Surv Asia* 7:11–20
- Muijsers JC, Weber Th, Van Hardeveld RM, Zandbergen HW (1995) Sulfidation study of molybdenum oxide using MoO₃/SiO₂/Si(100) model catalysts and Mo³⁺-sulfur cluster compounds. *J Catal* 157:698–705
- Nakano K et al (2013) Deep desulfurization of gas oil over NiMoS catalysts supported on alumina coated USY-zeolite. *Fuel Process Technol* 116:44–51
- Ninh TKT, Massin L, Laurent D, Vriant MA (2011) New approach in the evaluation of the support effect for NiMo hydrodesulfurization catalysts. *Appl Catal A: Gen* 407:29–39
- Patil SB, Mane SR, Patil VR, Kharade RR, Bhosale BN (2011) Chemosynthesis and characterization of electrochromic vanadium doped molybdenum oxide thin films. *Archiv Appl Sci Res* 3:481–491
- Pour AN, Rashidi AM, Jozani KJ, Mohajeri A, Khorami P (2010) Support effects on the chemical property and catalytic activity of Co-Mo HDS catalyst in sulfur recovery. *J Nat Gas Chem* 19:91–95
- Rana MS, Romirez J, Alejandre AG, Ancheyta J, Cedeno L, Maity SK (2007) Support effects in CoMo hydrodesulfurization catalysts prepared with EDTA as a chelating agent. *J Catal* 246:100–108
- Rashidi F, Sasaki T, Rashidi AM, Nemati Kharat A, Jafari Jozani K (2013) Ultradeep hydrodesulfurization of diesel fuels using highly efficient nanoalumina-supported catalysts: impact of support, phosphorus, and/or boron on the structure and catalytic activity. *J Catal* 299:321–335
- Roukoss C, Laurenti D, Devers E, Marchand K, Massin L, Vriant M (2009) Hydrodesulfurization catalysts: promoters, promoting methods and support effect on catalytic activities. *Comptes Rendus Chim* 12:683–691
- Saih Y, Segawa K (2003) Ultradeep hydrodesulfurization of dibenzothiophene (DBT) derivatives over Mo-sulfide catalysts supported on TiO₂-coated alumina composite. *Catal Surv Asia* 7:235–249
- Saleh TA (2011) The influence of treatment temperature on the acidity of MWCNT oxidized by HNO₃ or a mixture of HNO₃/H₂SO₄. *Appl Surf Sci* 257:7746–7751
- Saleh TA (2015) Isotherm, kinetic, and thermodynamic studies on Hg(II) adsorption from aqueous solution by silica-multiwall carbon nanotubes. *Environ Sci Pollut Res* 22:16721–16731
- Saleh TA, Danmaliki GI (2015) Influence of acidic and basic treatments of activated carbon derived from waste rubber tires on adsorptive desulfurization of thiophenes. *J Taiwan Inst Chem Eng*. doi:10.1016/j.jtice.2015.11.008
- Saleh TA, Gupta VK (2011) Functionalization of tungsten oxide into MWCNT and its application for sunlight-induced degradation of rhodamine B. *J Colloid Interface Sci* 362:337–344
- Saleh TA, Gupta VK (2012a) Photo-catalyzed degradation of hazardous dye methyl orange by use of a composite catalyst consisting of multi-walled carbon nanotubes and titanium dioxide. *J Colloid Interface Sci* 371:101–106
- Saleh TA, Gupta VK (2012b) Synthesis and characterization of alumina nano-particles polyamide membrane with enhanced flux rejection performance. *Sep Purif Technol* 89:245–251
- Saleh TA, Gupta VK (2012c) Column with CNT/magnesium oxide composite for lead(II) removal from water. *Environ Sci Pollut Res* 19:1224–1228
- Saleh TA, Gupta VK (2014) Processing methods, characteristics and adsorption behavior of tire derived carbons: a review. *Adv Colloid Interface Sci* 211:93–101
- Saleh T A (2015b) Nanocomposite of carbon nanotubes/silica nanoparticles and their use for adsorption of Pb(II): from surface properties to sorption mechanism. *Desalination Water Treat* 1–15
- Saleh TA, Agarwal S, Gupta VK (2011) Synthesis of MWCNT/MnO₂ and their application for simultaneous oxidation of arsenite and sorption of arsenate. *Appl Catal B: Environ* 106:46–53
- Saleh TA, Al-Saadi AA, Gupta VK (2013) Adsorption of lead ions from aqueous solution using porous carbon derived from rubber tires: experimental and computational study. *J Colloid Interface Sci* 396:264–269
- Saleh TA, Al-Saadi AA, Gupta VK (2014) Carbonaceous adsorbent prepared from waste tires: experimental and computational evaluations of organic dye methyl orange. *J Mol Liq* 191:85–91
- Solis D, Klimova T, Ramírez J, Cortez T (2004) NiMo/Al₂O₃-MgO (x) catalysts: the effect of the prolonged exposure to ambient air on the textural and catalytic properties. *Catal Today* 98:99–108
- Solis D, Ramirez J, Cuevas R, Contreas R, Cortez T, Aguilar M (2007) Synthesis and characterization of CoMo/Al₂O₃-MgO-(X) catalysts doped with alkaline oxides (K, Li). *Superf y Vacio* 20:19–26
- Sun Y, Prins R (2009) Mechanistic studies and kinetics of the hydrodesulfurization of dibenzothiophene on Co-MoS₂/γ-Al₂O₃. *J Catal* 267:193–201
- Talrose V, Yermakov AN, Usov AA, Goncharova AA, Leskin AN, Messineva NA, Trusova NV, Efimkina MV (2015) UV/Visible Spectra, NIST Chemistry WebBook, NIST Standard Reference Database Number 69, Eds. PJ Linstorm, WG Mallard 20899 <http://webbook.nist.gov>. Accessed 7 Apr 2015
- Tamura M, Shimizu K, Satsuma A (2012) Comprehensive IR study on acid/base properties of metal oxides. *Appl Catal A: Gen* 433–434:135–145
- Topsøe H, Hinnemann B, Nørskov J, Lauritsen J, Besenbacher F, Hansen P, Rasmus G, Egeberg G, Knudsen K (2005) The role of reaction pathways and support interactions in the development of high activity hydrotreating catalysts. *Catal Today* 107–108:12–22
- Trejo F, Rana MS, Ancheyta J (2008) CoMo/MgO-Al₂O₃ supported catalysts: an alternative approach to prepare HDS catalysts. *Catal Today* 130:327–336
- Villalón PC, Ramírez J, Cuevas R, Vázquez P, Castaneda R (2015) Influence of the support on the catalytic performance of Mo, CoMo, and NiMo catalysts supported on Al₂O₃ and TiO₂ during the HDS of thiophene, dibenzothiophene, or 4,6-dimethyldibenzothiophene. *Catal Today*. doi:10.1016/j.cattod.2015.06.008



- Wang Q, Hanson J, Frenkel AI (2008) Solving the structure of reaction intermediates by time-resolved synchrotron x-ray absorption spectroscopy. *J Chem Phys* 129:234502
- Wu L, Jiao D, Wang J, Chen L, Cao F (2009) The role of MgO in the formation of surface active phases of CoMo/Al₂O₃-MgO catalysts for hydrodesulfurization of dibenzothiophene. *Catal Commun* 11:302–305
- Zdrazil M, Klicpera T (2001) High surface area MoO₃/MgO: preparation by reaction of MoO₃ and MgO in methanol or ethanol slurry and activity in hydrodesulfurization of benzothiophene. *Appl Catal A: Gen* 216:41–50

